



Monitoring of jökulhlaups and element fluxes in proglacial Icelandic rivers using osmotic samplers



Morgan T. Jones^{a,b,*}, Iwona M. Gałeczka^a, Athanasios Gkritzalis-Papadopoulos^c, Martin R. Palmer^d, Matthew C. Mowlem^d, Kristín Vogfjörð^e, Þorsteinn Jónsson^a, Sigurður R. Gíslason^a

^a Institute of Earth Sciences, University of Iceland, Sturlugata 7, 101 Reykjavík, Iceland

^b Centre for Earth Evolution and Dynamics (CEED), University of Oslo, P.O. Box 1028 Blindern, 0315 Oslo, Norway

^c Flanders Marine Institute (VLIZ), Wandelaarkaai 7, 8400 Oostende, Belgium

^d National Oceanography Centre, University of Southampton Waterfront Campus, European Way, Southampton SO14 3ZH, UK

^e Icelandic Meteorological Office (Veðurstofa Íslands), Bústaðavegi 9, 150 Reykjavík, Iceland

ARTICLE INFO

Article history:

Received 17 October 2014

Accepted 29 December 2014

Available online 7 January 2015

Keywords:

Osmotic sampler
Jökulhlaups
Subglacial volcanoes
River monitoring
Element fluxes
Futurevolc

ABSTRACT

The quantification of volatile emissions from volcanoes is an integral part of understanding magmatic systems, with the exsolution and extent of volcanic degassing having a large impact on the nature of an eruption. Measurements of volatiles have traditionally focused on gas emissions into the atmosphere, but volatiles can also become dissolved in proximal water bodies *en route* to the surface. Thus the monitoring of rivers draining active volcanic areas can provide insights to identifying changes in activity. This process is particularly important for sub-glacial volcanoes in Iceland, where much of the volatile release is transported within glacial outbreak floods, termed jökulhlaups. Monitoring and characterising these phenomena is hampered by the dependence on spot sampling of stochastic events under challenging field conditions, which often leads to bias in the collected data. A recent technological advance is the osmotic sampler, an electricity-free pump that continuously collects water that can subsequently be divided into time-averaged samples. This technique allows for continued and unsupervised deployment of a sampler for weeks to months, representing a cost-efficient form of chemical monitoring. In this study we deployed osmotic samplers in two rivers in southern Iceland. Skálm is a proglacial river from Mýrdalsjökull glacier and Katla volcano, while Skaftá is a larger drainage system from the western part of Vatnajökull glacier. Both rivers are prone to jökulhlaups from geothermal and volcanic sources, and a small jökulhlaup of geothermal origin occurred during the second deployment in Skaftá in January 2014. The two deployments show that osmotic samplers are capable of delivering accurate chemical data in turbulent conditions for several key elements. Total dissolved fluxes for the deployment at Skaftá are calculated to be Na = 9.9 tonnes/day, Mg = 10.5 t/d, Si = 34.7 t/d, Cl = 11.0 t/d, Ca = 31.6 t/d, DIC = 50.8 t/d, and SO₄ = 28.3 t/d, with significant elevations of element concentrations during the jökulhlaup. Dissolved fluxes vary considerably on temporal scales from days to seasons, so that spot sampling may miss pulses in concentrations. This is particularly important for elements such as Mn. The continuous geochemical records from the osmotic samplers make it possible to identify pulses of fluxes attributed to sea spray, groundwater, and subglacial sources. The samplers can also be combined with existing methods of river monitoring, such as conductivity and discharge, to accurately assess changes to fluvial chemistry due to volcanic inputs. Moreover, there is the potential to deploy osmotic samplers in a range of other affected water bodies (e.g. wells, springs, lakes) to gain further insights into volcanic processes.

© 2015 Elsevier B.V. All rights reserved.

1. Introduction

In Iceland, the combination of abundant volcanism and high latitude climate results in the presence of subglacial volcanic systems. The chemical composition of rivers flowing from subglacial volcanoes is of interest for several reasons. Firstly, the release of magmatic volatiles

provides insights into the current state and life cycle of a volcanic system. Volatile release occurs through passive degassing at dormant volcanoes, long-lived geothermal systems, and during periodic eruptions. It is particularly relevant in the context of this study that eruptions can be preceded by a change in both volume and chemistry of emissions (Duffell et al., 2003; Aiuppa et al., 2007; Edmonds, 2008; Moretti et al., 2013), which also provide constraints on the style of eruption (Roggensack et al., 1997; Burgisser et al., 2008; Edmonds, 2008). Changes in volatile release during volcanic activity influence both groundwater and surface water chemistry (Aiuppa et al., 2000;

* Corresponding author at: Centre for Earth Evolution and Dynamics (CEED), University of Oslo, P.O. Box 1028 Blindern, 0315 Oslo, Norway.
E-mail address: m.t.jones@geo.uio.no (M.T. Jones).

Flaathen and Gislason, 2007; Varekamp, 2008; Jones et al., 2011). For subglacial volcanoes, much of the element release is into the subglacial rivers and springs due to the confining pressure of the overlying ice restricting release as gaseous volatiles (Gislason et al., 2002; Stefánsdóttir and Gislason, 2005).

Secondly, the melting of glaciers from underlying volcanic sources can lead to glacial outbreak floods, termed jökulhlaups. The two main causes of jökulhlaups are: (1) geothermal areas continuously melting an overlying glacier, leading to the accumulation and periodic draining of a subglacial lake; and (2) rapid melting of a glacier during a volcanic eruption through magma–ice interaction (Gudmundsson et al., 1997, 2008; Maizels, 1997; Kristmannsdóttir et al., 1999; Geirsdóttir et al., 2000; Gislason et al., 2002; Björnsson, 2003; Alho et al., 2005; Stefánsdóttir and Gislason, 2005; Russell et al., 2006, 2010). The former are more common and generally of lower magnitude. Peak discharges for subglacial lake-draining events are in the order of $100\text{--}2500\text{ m}^3\text{ s}^{-1}$. While these jökulhlaups are capable of washing away structures such as bridges, they are generally limited in terms of the extent and damage they cause. In contrast, volcanically triggered jökulhlaups can be catastrophic. Floods initiated by the eruption of Katla in 1918, one of the most active volcanoes in Iceland, peaked at $300,000\text{ m}^3\text{ s}^{-1}$ (Tómasson, 1996), while Holocene jökulhlaups draining to the north of Vatnajökull have been estimated to have had peak discharge rates of up to $700,000\text{ m}^3\text{ s}^{-1}$ (Waït, 2002). Hence, it is critical that these phenomena are properly understood, so that eruption response protocols are as accurate and well-informed as possible. The chemical composition of flood waters is one of the few clear indicators of the mechanism that caused a jökulhlaup, as reaction path modelling using pH, alkalinity, and element concentrations can derive the chemical evolution of the flood water and therefore the duration of water–rock interaction (Galeczka et al., 2014). While jökulhlaup-prone rivers are currently monitored for conductivity, temperature, and/or water stage by the Icelandic Meteorological Office (IMO), this information is not able to differentiate between subglacial lake-outbreak jökulhlaups and volcanic jökulhlaups in all cases due to the competing effects of dilution by meltwater and alkalinity increase by volatile addition.

Thirdly, the high mass flux and distinct chemical composition of jökulhlaups (Tómasson, 1996; Gislason et al., 2002; Snorrason et al., 2002; Stefánsdóttir and Gislason, 2005; Galeczka et al., 2014) mean that they have the potential to play a significant role in the global geochemical cycles of elements. In particular, the high suspended particulate flux of large jökulhlaups significantly increases the water-borne particulate flux to the ocean (Gislason et al., 2006a), and an increasing number of recent studies have shown that particulate material remains reactive in the ocean, playing an integral role in the biogeochemical cycles of a number of key elements (Lacan and Jeandel, 2005; Stefánsdóttir and Gislason, 2005; Arsouze et al., 2009; Jones et al., 2012a, 2012b, 2014; Singh et al., 2012; Pearce et al., 2013).

Jökulhlaups have been studied in detail with respect to their role in natural hazards, dissolved and particulate material transport, and fluid mechanics (Gudmundsson et al., 1997; Maizels, 1997; Kristmannsdóttir et al., 1999; Geirsdóttir et al., 2000; Gislason et al., 2002; Björnsson, 2003; Alho et al., 2005; Stefánsdóttir and Gislason, 2005; Russell et al., 2006, 2010). Monitoring the fluid discharge is complicated by the violence and inaccessibility of jökulhlaups, with monitoring stations often washed away by the deluge (Galeczka et al., 2014). The traditional method of river monitoring for chemical analyses has been spot sampling, as this method allows for the collection of large volume samples that can be analysed for multiple species. The major drawback of such sampling (in addition to the safety considerations) is that river systems and biogeochemical cycles vary over a wide range of temporal scales (Jannasch et al., 2004). Therefore, spot sampling on frequencies lower than those of the signal variations leads to a poor characterisation of the true signal, often missing significant stochastic events (Johnson and Jannasch, 1994; Dickey et al., 1997). The reason why

spot-sampling is *de rigueur* for much of the geochemical community is largely due to the availability of resources. Sites of interest may be logistically challenging to access, often needing good connections by car, boat, and/or proximity to civilisation. Associated costs of person hours, transport, electricity, and sampling equipment quickly become prohibitively expensive. Therefore, a cost-effective method of high-resolution sampling would be of great benefit for identifying volcanic components dissolved in rivers, how this signal varies with time, and as a precursory signal for a possible eruption during times of volcanic unrest.

A potential solution is the use of continuous sampling techniques. Historically, remote samplers were limited to tens of samples, or limited to a few dissolved constituents in the case of *in situ* samplers. A recent breakthrough is the development of osmotic samplers, able to collect continuous water samples without electricity from days to months at a time (Fig. 1; Gkritzalis-Papadopoulos et al., 2012a, 2012b; Jannasch et al., 2004). Osmotic samplers have been successfully deployed on an abyssal plain (Jannasch et al., 2004) and in a low-discharge river (Gkritzalis-Papadopoulos et al., 2012b), delivering accurate element concentrations over short time-averaged intervals. However, these samplers have never been tested in a dynamic and occasionally violent system such as a proglacial river from a subglacial volcano. In this study we deployed osmotic samplers in two rivers in southern Iceland during 2013 and 2014. Both rivers are periodically affected by jökulhlaups from both volcanic and geothermal sources. The first river, Skálm, is a short proglacial river flowing out from the east of Mýrdalsjökull, the glacier covering much of the Katla volcanic system (Fig. 2). There are numerous cauldrons within the central caldera, each capable of producing geothermally driven outbreak floods in addition to the periodic volcanogenic jökulhlaups from Katla eruptions. The second river, Skaftá, is part of a larger catchment that includes meltwater from Vatnajökull glacier and has periodic geothermal jökulhlaups from the Skaftár cauldrons in the western part of this glacier (Fig. 3). Volcanic jökulhlaups in this catchment could potentially be driven by an eruption of Hamarinn, Grímsvötn, and/or Bárðarbunga volcanoes, although there are no historic examples of this occurrence. Therefore, the two target catchments display sufficient variation to be an ideal test of osmotic samplers in challenging and turbid fluvial conditions.

2. Methods

2.1. Osmotic sampler

Two osmotic pumps were custom built by the Sensors Development Group at the University of Southampton and Quayside Precision Engineering, Southampton (Fig. 1). The sampler consists of two chambers separated by multiple osmotic membranes (Theeuwes and Yum, 1976). The upper chamber is filled with NaCl salt and de-ionised water to form a supersaturated brine in which some salt remains as a solid phase in the chamber. The lower chamber is filled with pure de-ionised water to create a strong ionic gradient between the two chambers. The osmotic membranes exclude passage of dissolved salts, so flow of fluid is only permitted from the freshwater chamber to the brine chamber. Under-pressure created in the fresh water compartment continuously draws water up into a long small-bore Teflon tube attached to the lower chamber. This tubing then stores the sample until collection, with processing in the laboratory involving division of the tubing into time-averaged samples and subsequent chemical analyses. The continuous nature of this sampling does not bias between diurnal and nocturnal collection, or between calm and inclement weather conditions, a common flaw with spot sampling. Deployment times can be from weeks to years, while having the benefit of being automatic, electricity-free, and cost effective (Gkritzalis-Papadopoulos et al., 2012a). A limiting factor is the small size of the sample retrieval with short time increments, typically $<1\text{ ml}$ per day. While some analyses such as metal isotopes are ruled out, this sample volume still allows

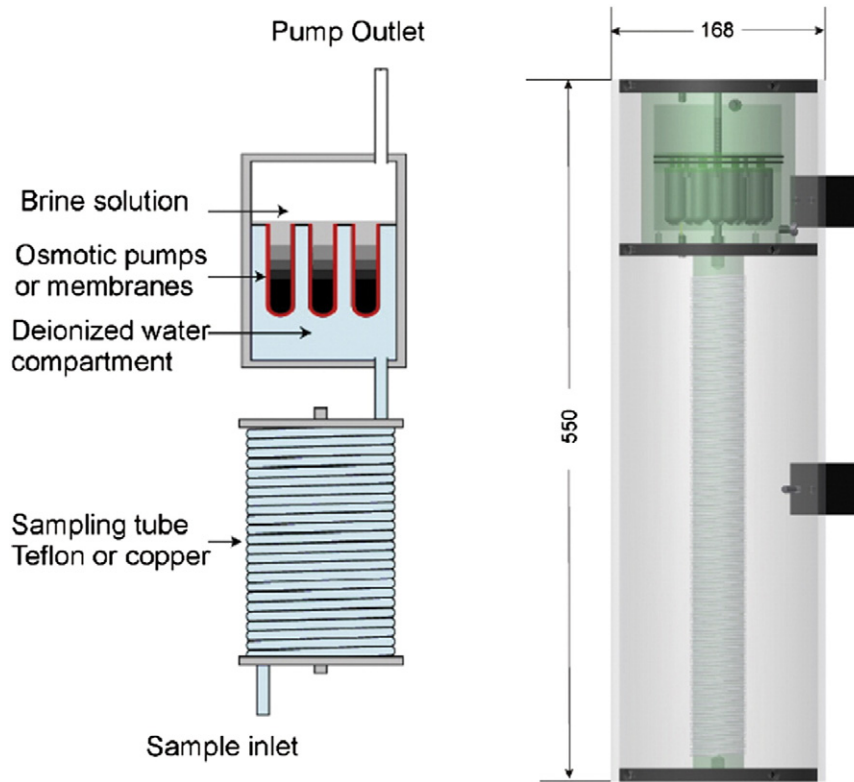


Fig. 1. A schematic illustration of the osmotic samplers deployed in this study. The left-hand illustration shows the principle of design. The right-hand picture is a CAD model of the samplers developed at the National Oceanographic Centre, Southampton. Dimensions are in mm.

for the measurement of many dissolved constituents averaged over a short time period.

The magnitude of the salt gradient between the two chambers (a function of the concentration difference), the temperature dependent

solubility of NaCl, the diffusive constant for H₂O, and the thickness of the osmotic membrane are directly related to the subsequent osmotic pressure and the resulting flow rate between the chambers. The osmotic pressure is maintained by keeping the brine solution saturated with

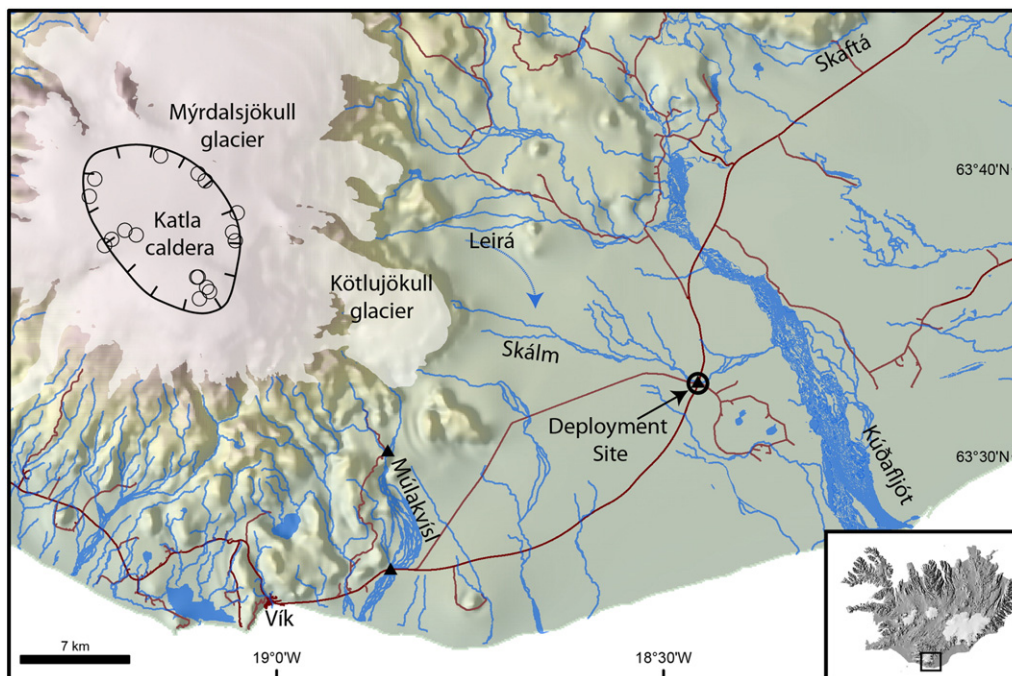


Fig. 2. A map of southern Iceland showing Katla volcano, Myrdalsjökull glacier and the associated proglacial river systems. Black triangles denote hydrological monitoring stations operated by the Icelandic Meteorological Office (IMO). Small circles on Myrdalsjökull denote current subglacial geothermal cauldrons. The blue arrow denotes the direction of the rechanneling of part of the Leirá River into the Skálm catchment in July 2013. Roads are shown as red lines.

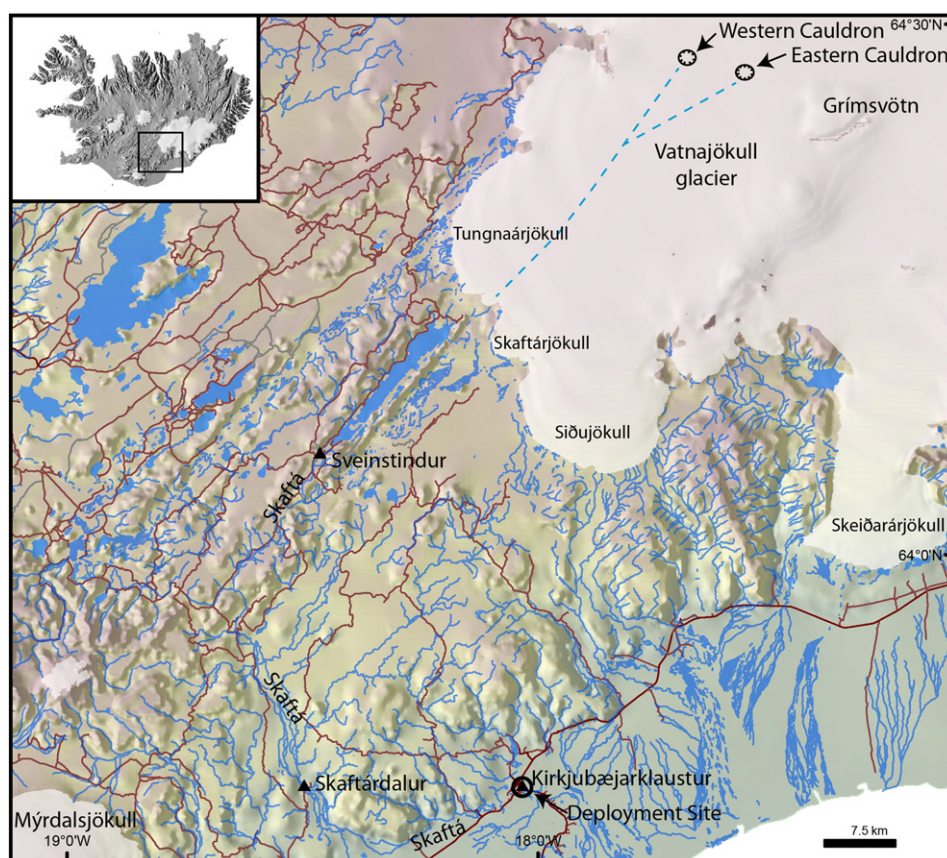


Fig. 3. A map of southern Iceland showing the Skaftá river system originating from under the Vatnajökull glacier. The black triangles label the hydrological monitoring stations operated by the IMO on this river. The dashed blue line approximates the subglacial channels from the Skaftár cauldrons. Roads are shown as red lines.

excess salt. This continuous fluid collection is remarkably stable in terms of flow rate, only varying markedly with temperature. The flow rate of each osmotic membrane, as provided by the company Alzet, is determined by:

$$Q = Q_0 \left(0.141e^{0.051T} - 0.007\pi + 0.12 \right) \quad (1)$$

where Q_0 is the specific flow rate for the osmotic pump at 37 °C ($10 \mu\text{L h}^{-1}$), while π is the osmolality (bar) of the solution outside the membrane. For the setup deployed in this study, $\pi = 0$ (Gkritzalis-Papadopoulos et al., 2012a). Coupled with a record of ambient temperature, this equation can be used to predict the flow rate as a function of time, and therefore sample age as a function of location in the sample tubing. The temperature range in southern Iceland should correlate to about 22–40 m of sample collected in the tubing per month, around 80–133 cm for a daily-averaged sample. Water flow within the sample tube is purely laminar and the internal mixing of the collected sample by diffusion in the Teflon tube is only ~2–3 cm per month (Gkritzalis-Papadopoulos et al., 2012a). Therefore, a daily-averaged sample from modified osmotic samplers used here, collected a month after installation, has a ~5% error from diffusive mixing with the adjacent daily-averaged samples.

2.2. Skálm field deployment

The first installation of the osmotic samplers was from April until August 2013 in Skálm River, one of several proglacial rivers to the east of Mýrdalsjökull glacier and the underlying Katla volcano (Fig. 2). Katla has an eruption roughly twice a century (Larsen, 2000; Óladóttir

et al., 2008), typified by explosive subglacial eruptions that produce widespread tephra layers and sizeable jökulhlaups (Thordarson and Larsen, 2007; Óladóttir et al., 2008). The last major volcanic eruption with an associated large jökulhlaup occurred in 1918 (Tómasson, 1996), while the last geothermally triggered subglacial lake-outbreak jökulhlaup occurred in 2011 (Galeczka et al., 2014). Skálm River is fed from a mixture of spring, glacial, and meteoric sources. During the winter months, the river flow rate is low and dominated by spring water. In summer months, discharge increases due to melt water from Mýrdalsjökull glacier. The catchment is also occasionally affected by jökulhlaups from the Katla volcano and associated geothermal systems. The main fluvial outflow for these outburst floods is the more southerly Múlakvísl River (Russell et al., 2010), but the unpredictable migration of the channel makes this river unsuitable for sampler deployment.

The bridge crossing of Route 1 over Skálm is only at risk of total inundation during a large eruption from Katla, so it was chosen as the preferred initial installation over other proglacial rivers east of Mýrdalsjökull. Data on water stage, temperature, and conductivity are constantly monitored by the hydrological network of the IMO at this location, allowing for the direct integration of this existing monitoring data with that acquired from the continuous osmotic samplers. The sampler was anchored to the bottom of the river by hammering a pole into the sediment beneath the bridge, to which the sampler was then attached (Fig. 4). The sample tubing was changed monthly, while spot samples were taken 2–4 times per month to calibrate and corroborate the results from the sampler. The installation at Skálm ended when the powerful Leirá River tributary was rechanneled into the Skálm catchment towards the end of July 2013 (Fig. 2). The bottom anchoring method of securing the sampler led to the inundation and eventual

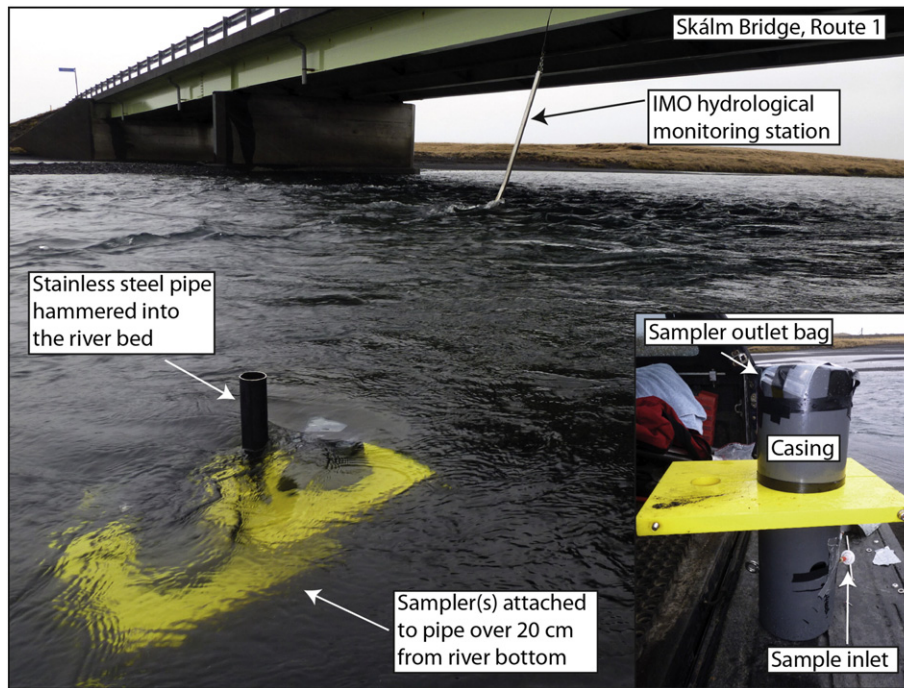


Fig. 4. The installation of the osmotic samplers in the Skálm River from April until August 2013, facing southwest.

burial of the sampler by the sharp increase in sediment flux. This change in field conditions meant that the Skálm sample site was unsuitable for further monitoring.

2.3. Skaftá field deployment

The second sampling station is on the Skaftá River at the town of Kirkjubæjarklaustur, where deployment began in November 2013 until July 2014 (Fig. 3). This river is of interest because it is affected by two subglacial lakes under the western and eastern Skaftár cauldrons on the west side of Vatnajökull glacier. Elevated geothermal activity causes basal melting of the glacier, with water accumulating in two

subglacial lakes beneath the cauldrons. Periodically these lakes feed glacial outburst floods, affecting the whole of the Skaftá River. The location of sampler deployment is ideal because: (1) small to moderate jökulhlaups are a common phenomenon here (Björnsson, 1977; Zóphóníasson, 2010); (2) there are three continuous hydrological monitoring stations at Kirkjubæjarklaustur, Skaftárdalur and at Sveinstindur for water stage, conductivity (except Kirkjubæjarklaustur), and temperature, operated by the IMO; (3) the bridge at Kirkjubæjarklaustur is easily accessible and the bridge supports offer protection against high water discharge events; and (4) anthropogenic influence on the catchment is low. Skaftá has also been the focus of previous investigations of jökulhlaups, measuring discharge, suspended sediment dynamics,

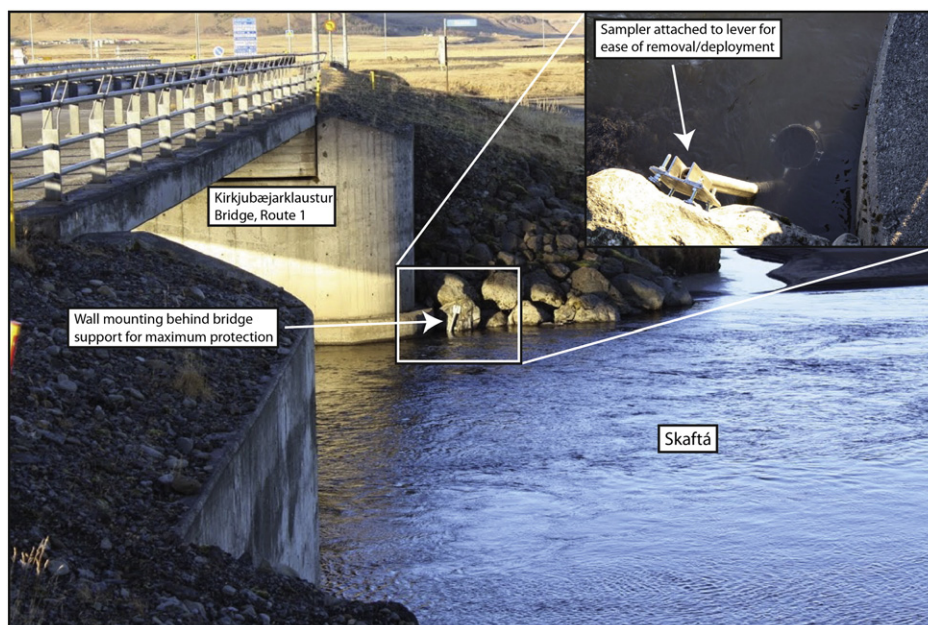


Fig. 5. The installation of the osmotic samplers in the Skaftá River from November 2013 until July 2014, facing north.

chemistry of dissolved and suspended matter, and electrical conductivity (Elefsen et al., 2002; Old et al., 2005; Gislason et al., 2006b). The samplers were deployed through attachment to the bridge side wall support, clear of the river bottom (Fig. 5). Spot samples that served as control samples were collected periodically on a much greater frequency than the Skálm deployment. A small subglacial lake outbreak flood occurred in January 2014. During this flood, control samples were taken daily (20–24 Jan. and 29 Jan.–5 Feb.), then every other day (5–28 Feb.), and finally twice a week until the end of the deployment (6 July).

2.4. Laboratory analyses

Spot samples were collected into 1 L HDPE bottles and refrigerated at $\sim 2^\circ\text{C}$ until further treatment. In the laboratory, the samples were filtered through $0.2\ \mu\text{m}$ Millipore cellulose acetate membranes into acid washed HDPE tubes for cations and trace metal analyses, and into LDPE bottles for anions. Samples for major and trace element analyses were acidified using Suprapur® 0.5% (v/v) HNO_3 . Conductivity, alkalinity and pH were measured immediately after filtration. Filtering of samples was conducted as soon as possible upon return to the laboratory, typically 4–10 h after collection. Towards the end of the Skaftá field study, samples were filtered *in situ* 10–30 min after collection. Dissolved F^- , Cl^- , SO_4^{2-} , and NO_3^- concentrations were quantified using an IC-2000 Dionex, ion chromatograph. Flow precision and accuracy on this machine are $<0.1\%$. Manual peak fitting for concentrations measured here results in a maximum $\pm 2\%$ error for each element with the exception of F, which has a maximum error of $\pm 5\%$. Cations and trace metals were measured using a Spectro Cirrus Vision inductively coupled plasma, optical emission spectrometer (ICP – OES), with an in-house standard, and checked against the SPEX Certified Reference Standard. Associated analytical errors are $<5\%$ for ICP analyses, including uncertainties obtained through sample dilution.

The continuous osmotic samples were collected through a $0.45\ \mu\text{m}$ cellulose acetate filter attached to the tubing coil in the field. Sample tubing was collected and replaced on a monthly basis from the deployed osmotic samplers. The sample was then taken straight to the laboratory for processing. The sample tubing was cut into 1 m segments (corresponding to $\sim 0.81 \pm 0.02\ \text{ml}$ fluid) and each aliquot transferred to high-density polypropylene sample tubes. The number of 1 m samples was then back calculated using the length of the sampler deployment to ascertain the time duration of each 1 m sample. This varied between 19 and $22\ \text{h m}^{-1}$ for the Skálm installation and $18\text{--}31\ \text{h m}^{-1}$ for the Skaftá installation, with faster flow rates in warmer conditions. There is a close correlation between flow rates calculated from Eq. (1) using IMO water temperature data and the observed flow each month. For the Skálm installation and the beginning of the Skaftá installation, each aliquot was then diluted approximately 10–14 times with de-ionised water that had been acidified with Suprapur® 1.0% (v/v) HNO_3 . The dilution was to provide sufficient sample to conduct the necessary analyses. At the end of the Skálm installation and for the Skaftá installation, there were sporadic concerns that the inlet filters on the sample tubing in the field did not completely filter the inlet solutions. In these cases, the sample was diluted with pure de-ionised water, filtered in the laboratory, and then acidified.

The Skálm deployment is divided into 3 stages based on each round of deployment: (1) 19 Apr.–27 May 2013, (2) 27 May–1 July, (3) 1–31 July. Each change of sampler is marked as a grey line on Fig. 6. For each stage every aliquot was diluted $\sim 10\text{--}14$ times with pre-acidified water. Only cations were measured from this deployment. The Skaftá deployment is divided into 6 stages based on each deployment: (1) 13 Nov.–20 Dec. 2013, (2) 20 Dec. 2013–24 Jan. 2014, (3) 24 Jan.–28 Feb., (4) 28 Feb.–14 Apr., (5) 14 Apr.–25 May, (6) 25 May–6 July. Again, each change of sampler is marked as a grey line in Fig. 7. Stage (1) was run with the same procedure as at Skálm. Stage (2) aliquots were diluted with DI water then a 2 ml subsample was transferred to

HDPP sample tubes for analysis of anions with ion chromatography (IC-2000). The remaining solutions were acidified with 0.5% (v/v) HNO_3 . For stages (3) to (6), the diluted water was first filtered through $0.2\ \mu\text{m}$ cellulose acetate membranes to remove suspended particles which could have entered the tubing through the joints of the tubing and filter, while also being comparable to the control samples filtered with a $0.2\ \mu\text{m}$ filter. The analytical procedure then followed stage (2). For stage (6), spot samples were filtered on site to assess whether the storage and transit time between Kirkjubæjarklaustur and Reykjavík impacted the measured sample chemistry. There were several logistical challenges associated with these deployments, as detailed in the Supplementary data.

3. Results

3.1. Skálm field deployment

The results of the Skálm installation are summarised in Fig. 6 and in the Supplementary material. The mean pH of spot samples is 7.79 ($\sigma = 0.10$), with little variation throughout the installation period. The water stage and conductivity data from the IMO's hydrological station indicates three broad phases of the river during the course of the installation. Until late May, the river was dominated by spring and meteoric sources, typified by little variation in water stage and conductivity independent of the diurnal temperature variations. From late May until late July, Skálm displays an increasing proportion of runoff from snow and glacial melting, as evidenced by an increase in total runoff and marked diurnal variations in electrical conductivity. At the end of July, the powerful Leirá River changed course (as shown by the arrow in Fig. 2) and part of the flow channelled into the Skálm catchment, leading to an abrupt increase in runoff. Conductivity also increased as Leirá has a high component of water derived from the northern Katla subglacial cauldrons (Fig. 2). This rechanneling led to the burial of the osmotic sampler around the 24th July, and the discontinuation of the installation at this location shortly after.

The data collected from spot samples (dots in Fig. 6) correlates well with the data obtained from the continuous osmotic samplers (lines in Fig. 6). Each element shows a small range in measured concentrations, with the exception of the sample taken on the 1st August that has elevated dissolved components from the addition of Leirá waters. The daylight collection of this spot sample is distinctly different from daily averaged sample, evidenced by elevated dissolved concentrations of Na, Ca, Si, Mn, and SO_4 in the spot sample. This underlines the fact that spot sampling can lead to acquisition of unrepresentative data. Statistical analyses to compare variance between the spot samples and the continuous samples are not possible due to an insufficient control sample dataset. It is apparent, however, that the continuous osmotic samples identified several pulses of element fluxes that were not recorded by the sporadic collection of control samples. Moreover, the temporal resolution and the consideration of several co-varying elements from the time-integrated samples allows for individual events from several distinct sources to be identified. This effect is clearly observable at this locality due to the small catchment area and short distance from the glacier, leading to less mixing of tributaries that might dampen such signals.

3.2. Skaftá field deployment

- Characterisation of Skaftá River in a 'neutral' state

The results of the sampling station on the Skaftá River are shown in Fig. 7 and in the Supplementary material. The mean pH of spot samples is 7.58 ($\sigma = 0.52$). The background variability of the river chemistry is less than at Skálm due to the difference between the two catchments. Skálm is a short proglacial river that responds quickly to variations in

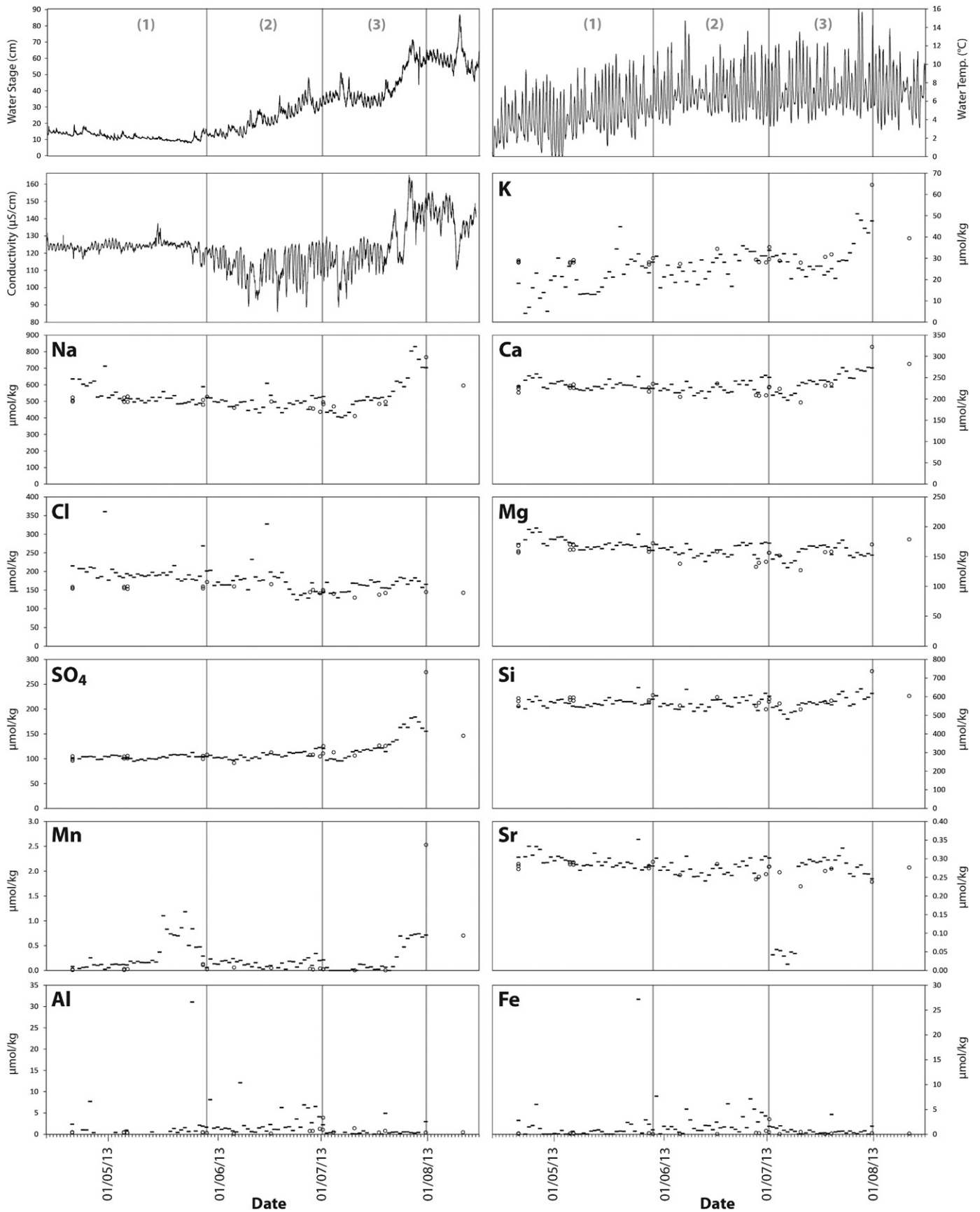


Fig. 6. Selected dissolved element concentrations from the deployment of the osmotic samplers at Skálm River between April and August 2013. Results from the daily-averaged continuous osmotic samplers are shown as flat lines covering the time that is averaged for each sample, while the corresponding dots refer to spot samples taken at that location. Water stage, temperature and electrical conductivity were measured by the Icelandic Meteorological Office's (IMO) hydrological station at Skálm Bridge (IMO, 2013). The lines subdivide each deployment of the osmotic sampler.

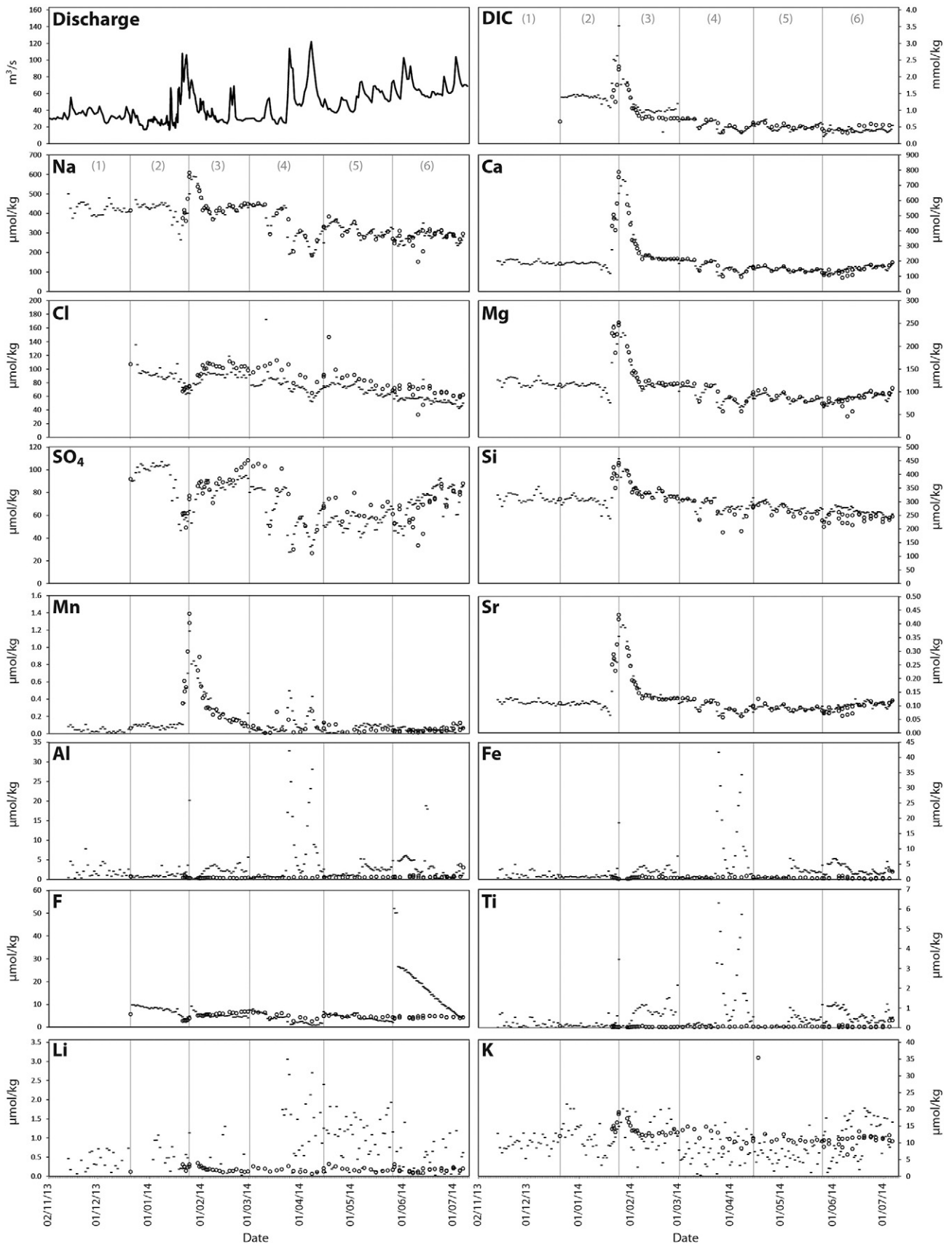


Fig. 7. Selected dissolved element concentrations from the deployment of the osmotic samplers at Kirkjubæjarklaustur from November 2013 until July 2014. Results from the daily-averaged continuous osmotic samplers are shown as flat lines covering the time that is averaged for each sample, while the corresponding dots refer to spot samples taken at that time. The grey lines divide each stage of deployment (1–6). Discharge was measured by the IMO at the same location. From 20th December 2013 to 10th February 2014, the discharge data is hourly and has been manually checked (IMO, 2014a). All other data is unchecked daily discharge rates (IMO, 2014b).

Table 1
Statistical mean difference (in %) and standard deviation (σ) between the dissolved element concentrations of spot samples and the corresponding time-averaged samples for the Skaftá river. The 'neutral' values refer to the normal state of the river; the 'jökulhlaup' values are the mean differences between the sample sets from 20th January until 7th February 2014.

		Si	Na	K	Ca	Mg	Fe	Al	Sr	Mn	Ti	DIC	Cl	SO ₄	F
Neutral	Mean diff. (%)	5.1	-3.4	-78.0	-1.6	-4.1	-57	62	-3.2	-50.6	72	-7.7	-23.1	-12.3	-14.5
	s.d. (σ)	6.7	16.0	133.2	12.1	10.8	737	49	13.7	351.7	196	35.3	16.2	30.4	71.2
jökulhlaup	Mean diff. (%)	-1.4	-1.9	13.7	-8.3	0.8	-673	-673	-5.7	-4.3	-1344	-27.4	8.1	4.1	-33.0
	s.d. (σ)	8.4	6.6	29.7	17.2	11.3	2065	1504	16.6	36.6	2516	36.7	9.5	10.3	42.1

source fluxes, whereas the Skaftá site lies at the confluence of several catchments that span a wide section of the southern Icelandic highlands. Therefore, minor changes in fluxes are dampened and spread over several days, making their detection more difficult. The water stage measured by the IMO's hydrological station indicates two broad phases of the river during the course of the installation. Until late March, the water background discharge was $\sim 25 \text{ m}^3 \text{ s}^{-1}$ and the water was mainly of spring and meteoric origin. From late March until July, Skaftá displayed an increasing proportion of runoff from snow and glacial melting, as evidenced by an increase in background discharge to $\sim 45 \text{ m}^3 \text{ s}^{-1}$.

As with the previous installation at Skálm, major element concentrations in Skaftá compare well between the spot samples and continuous samples (Fig. 7). However, due to the much higher frequency of spot sampling, a meaningful statistical analysis of the two data sets is possible. Silica, Na, Ca, Mg, Sr, and DIC show low (<8%) mean differences between the two datasets with relatively low standard deviations (Table 1). The Cl, SO₄ and F anions display slightly greater variation, while the two sample sets differ considerably for elements such as K, Fe, Al, Mn, and Ti. There is a general trend of decreasing element concentrations during spring and early summer that is likely due to the dilution of ground/spring water by the melting glacier. From March 2014 onwards, large fluctuations in discharge were measured (Fig. 7). The elemental concentrations in both sampling methods and conductivity measured at Sveinstindur fluctuate concomitantly with precipitation events, with little to no input of subglacial meltwater during this period. For example, increased discharge around 25th March and 8th April 2014 correlates with decreases in most elemental concentrations, suggesting a dilution from meteoric water. The exceptions are redox sensitive elements Fe and Mn, and the more immobile elements Al and Ti, which increase during peak discharge events. Despite the increased frequency of spot sample collection, the episodes of substantial increases in Fe, Al, and Ti were missed by the spot samples, while elevated Mn concentrations were recorded in only one spot sample.

- Characterisation of the Skaftá River during a minor glacial flood

During the Skaftá deployment a minor jökulhlaup occurred, originating from one of the Skaftár cauldrons, and was channelled into the Skaftá River. The first signs of a glacial flood were observed as increased discharge at the IMO's Sveinstindur hydrological monitoring station (Fig. 3) on 18th January 2014. Visual observations of the Vatnajökull glacier showed that the flood originated from the western Skaftár cauldron, which last drained in September 2012. The peak discharge of Skaftá observed at Sveinstindur was $384 \text{ m}^3 \text{ s}^{-1}$ on 19th January 2014, larger than the measured discharge of $284 \text{ m}^3 \text{ s}^{-1}$ at this location during the 2012 flood. The following day, peak discharges were $\sim 200 \text{ m}^3 \text{ s}^{-1}$ at Skaftardalur, $110 \text{ m}^3 \text{ s}^{-1}$ at Ása Eldvatn and $100 \text{ m}^3 \text{ s}^{-1}$ at Kirkjubæjarklaustur. The peak discharge was diminished at Kirkjubæjarklaustur because Skaftá splits into two as it exits the highlands and also contributes to the Kúðafjót River (see Fig. 2). The mean pH of spot samples during the duration of the flood is 7.35 ($\sigma = 0.32$). The jökulhlaup was detected by both the spot samples and the continuous samples from the osmotic pump, as shown in Fig. 8. The chemical signal of the main phase of the jökulhlaup manifested as

marked peaks in several major cations such as Si, Na, Ca, Mg, and trace elements such as Sr, and Mn. Anion donors such as F, Cl, and SO₄ were lower than background concentrations during the winter period. The lack of significant F, Cl, and SO₄ increase, combined with high cation concentrations, is characteristic of a glacial flood originating from geothermal heat source melting the ice (Sigvaldason, 1963, 1965; Galeczka et al., 2014). Alkalinity and dissolved inorganic carbon (DIC) concentrations significantly exceeded background concentrations, confirming that the signal was derived from long term water–rock interaction prior to the flood and rules out a volcanic origin of the meltwater. During the jökulhlaup, acetate ($\text{C}_2\text{H}_3\text{O}_2^-$) was measured in both the spot and continuous samples. This species is indicative of microbial activity in the water prior to release into proglacial environments, and has also been found in flood waters originating from geothermal reservoirs (Galeczka et al., 2014). Moreover, microbiological activity has been found to occur in the Skaftá geothermal subglacial lakes (Martinson et al., 2013). Boron concentrations also show a peak in the spot samples (see Supplementary data), but B concentrations are close to the detection limit of the ICP-OES method ($0.93 \mu\text{mol/kg}$) in the diluted continuous samples. Boron is a highly mobile element, so elevated concentrations are further evidence of substantial water–rock interaction (Arnórsson and Andrésdóttir, 1995).

During the flood event, the mean differences between concentrations of measured elements in the spot samples and continuous samples continue to compare well for Si, Na, Ca, Mg, and Sr (Table 1). The correlation between measured concentrations of K, Mn, Cl, and SO₄ actually improve compared to background statistical data, for K and Mn this is because the increased fluxes of these elements lessen the error associated with measuring dilute waters close to the analytical detection limit. Comparisons of DIC and F become worse during the flood, with stochastic fluctuations leading to increased discrepancies between time-averaged and spot sampling. There are very poor comparisons between the two sample sets for Fe, Al, and Ti, with the difference between mean values exceeding 600% in each case (Table 1). The elemental discrepancies between the spot samples and the continuous samples are most acute at the beginning of the flood, where high temporal fluctuations in discharge are recorded.

4. Discussion

4.1. Sources of element flux pulses

There are occasional concurrent peaks in dissolved Na and Cl concentrations that are particularly pronounced on 29th April, 27th May, and 15th June 2013 during the Skálm deployment (Fig. 6) and on the 21st Dec 2013 during the Skaftá study (Fig. 7). Significant storm events with strong southerly winds occurred before each of these concurrent Na and Cl pulses, representing an influx of sea spray with associated salts into the catchments. As previously mentioned, identifying these events in Skaftá is complicated as the signal is dampened and diluted, making their detection more difficult. In Skálm, there are occasions when peaks in Na concentrations are not coupled with increases in dissolved Cl, but are concurrent with peaks in Si, Ca, and SO₄ (e.g. 28–30th June, Fig. 6). These events likely result from stochastic releases of water from subglacial sources that have experienced considerable fluid–rock interaction and have similar chemical compositions to geothermal sources

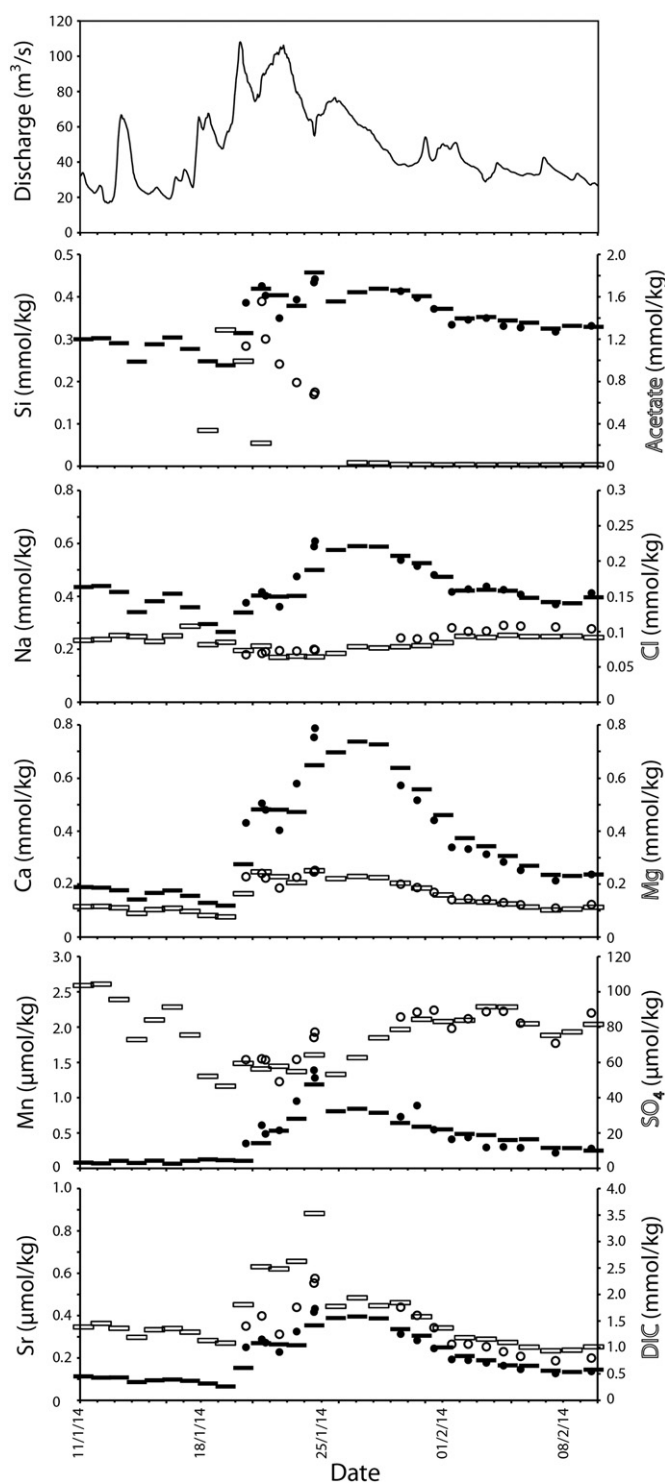


Fig. 8. Selected dissolved element concentrations from the deployment of the osmotic samplers in the Skaftá River at Kirkjubæjarklaustur between January and February 2014. Discharge is calculated from hydrological network data from the IMO station at Kirkjubæjarklaustur. Results from the time-averaged continuous osmotic samplers are shown as lines, while the dots refer to spot samples taken at that location. Open symbols refer to the right hand y-axes, while filled symbols refer to the left hand y-axes.

(Kaasalainen and Stefánsson, 2012). These elements also show considerably increased concentrations following the rechanneling of Leirá, suggesting a higher component of geothermally-sourced water in this river.

There are peaks in redox sensitive elements in both studies that occur in spring months. Dissolved fluxes of Mn at Skálmm from 16–27th May 2013 are considerably elevated in the river waters (Fig. 6). At

Skaftá, the fluxes of the redox sensitive elements Fe and Mn and the immobile elements Al and Ti are markedly increased during peak discharge events between 23rd–28th March and 3rd–9th April 2014 (Fig. 7). Pulses of this kind have been observed elsewhere in Iceland, which are caused by the build-up of snow and ice during winter months that leads to oxygen depletion in the underlying soils. The reduced conditions result in increased transition metal concentrations in interstitial soil waters. Thawing of soils and/or flushing during peak discharge events then transfer part of this elemental signature to fluvial waters (Eiriksdóttir et al., 2013b, 2014). Much of this stochastic signal is missed by the spot sampling.

4.2. Comparing continuous and spot samples

As the results from both deployments show, there is a strong correlation between the control samples and the daily-averaged continuous samples for Si, Na, Ca, Mg, Cl, SO_4 , Sr, and Mn. In contrast, there are significant differences between the measured concentrations of Fe, Al, and Ti for the two sample sets. Potassium appears to show some correlation in the Skálmm data, but poor correlation in the Skaftá data, primarily because the latter has low K concentrations that are close to the detection limit of the analytical method. For Li and NO_3 , there is markedly less variability in the daily-averaged continuous samples compared to the spot samples. Again, this is likely due to the fact that the concentrations of these elements commonly approach the analytical detection limit in the diluted osmotic samples, and cannot therefore be readily compared with the data from the spot samples.

An important consideration is that the lack of immediate filtration of the spot samples may lead to the dissolution of particulate material and the precipitation of secondary phases, both of which would affect element concentrations. Moreover, the presence of suspended particulate material in the large volume samples increases the possible reactive surface area on which secondary phases may precipitate. For stage 6 of the Skaftá deployment, control samples were filtered immediately after their collection to assess whether this affected the measured element concentrations. As can be seen in almost all the element patterns, the filtration does not significantly influence measured concentrations, although as with other deployments there were considerable differences in measured Fe, Al, and Ti observed in both the spot control and continuous samples (Fig. 7). Only three spot control samples out from the 13 that were filtered *in situ* gave a better fit with the data from the continuous samples. The concentrations of Fe, Al, Mn, and Ti are generally higher in the continuous samples than in the spot control samples, even when the latter were filtered *in situ*, but the lack of concomitant Si concentration increases in the continuous sample data suggests that this is not due to contamination from suspended particle dissolution. The most probable explanation is that collection by spot sampling leads to a rapid precipitation of poorly soluble elements that is more rapid than the 10–30 min it takes to complete *in situ* filtering. Since the main difference between the spot samples and continuous samples is the presence of suspended material, it is likely that the sediment is acting as the nuclei for precipitation.

Fluorine concentrations show the largest variability of the anions measured, although the variability in the spot samples follows the same general trend shown by the continuous samples, especially during the flood peak (Fig. 8). This discrepancy may be due to the analytical method of IC chromatography, where the F peak is the first to appear after the water dip. Defining the peak, and therefore the F concentrations, induces greater error in diluted waters such as those from the continuous samples. During the stage 6 deployment at Skaftá, the measured F concentrations from the continuous sampler were initially elevated ($\sim 50 \mu\text{mol kg}^{-1}$), before returning to background concentrations of $1\text{--}5 \mu\text{mol kg}^{-1}$ (Fig. 7). This effect was not seen in the control samples, suggesting that the initial high F concentrations may have been due to the use of a new reel of FEP tubing. High F concentrations were also measured in the DI water in the tubing

before sampling, as reflected in the earliest sample from each deployment having elevated F values. Moreover, F concentrations in previous stages increase with residence time in the tubing. According to the manufacturer (Polyflon), residual HF and volatile fragments can remain trapped in the tubing from the melting of fluoropolymers during the manufacture of the tubing, likely explaining this erroneous element data.

While the record of the continuous samples shows greater detail than the spot samples, there are some drawbacks associated with this method of sampling in a proglacial fluvial environment. The high-energy conditions abrade and deteriorate the pump fittings, while suspended sediment can clog the inlet filter that may change the flow rate into the tubing over time. Temperature has an effect on the pump flow rate, which means that a continuous temperature record is necessary to accurately time the events. These flow rate effects are also compounded with longer deployment times. The dilution of the small sample volumes to obtain a near daily-averaged sample means that some elements are below the limit of detection of the methods used here, including trace elements (B, Li, NO₃) and toxic metals (Cr, As, Pb).

4.3. Constraining fluvial element fluxes

The two datasets offer an insight into element fluxes from catchments affected by subglacial volcanism. A compilation of element fluxes from this study, other notable rivers in Iceland (Eiriksdottir et al., 2013a), and selected large global catchments (Gaillardet et al., 1999) are shown in Table 2. Both of the rivers studied here are richer in dissolved constituents than rivers in NE Iceland, most likely due to the higher component from geothermal sources. Aside from Si, which is more concentrated in Skálm and Skaftá, the average dissolved concentrations fall within the range of large global catchments (Gaillardet et al., 1999; Table 2). Combining the discharge data measured by the IMO at Kirkjubæjarklaustur and the continuous sample concentrations allows for the quantification of dissolved element fluxes in the Skaftá River. Selected daily fluxes are shown in Table 3. The most voluminous dissolved fluxes are DIC, Si, Ca, and SO₄, calculated at 50.8, 34.7, 31.6 and 28.3 tonnes/day during the period 13 Nov. 2013–6 July 2014, respectively. Sodium (9.9 t/day), Mg (10.5), and Cl (11.0) also represent significant daily fluxes of these elements. Both of these datasets clearly show that there are considerable temporal variations in fluxes from daily to seasonal scale. The Skaftá installation continued for nearly nine months, considerable enough for a daily flux estimate to be robust. However, in

the absence of autumnal sample collections, scaling these values to a yearly flux should be conducted with a degree of caution.

The continuous data collected on the minor Skaftá jökulhlaup observed in January 2014 can be used to make estimates of the total elemental flux contribution to the overall flux to the ocean from sporadic events such as glacial floods. The second and third rows of Table 3 show the calculated mean daily element fluxes during the jökulhlaup (defined as 19–28th January 2014 at Kirkjubæjarklaustur) and the 'background' flux (defined as the mean of all other daily samples). Comparisons of these two fluxes are noteworthy, especially for elements that are rich in the glacial outbreak fluids. Manganese is the most enriched element, with almost a 10-fold flux increase during the effect of the jökulhlaup. Despite later pulses of Mn in March and April from groundwater thawing, the Mn fluxes during the nine days after the jökulhlaup led to the mean flux from the duration of the installation being 33% higher than the background flux. Dissolved inorganic carbon was over 6 times higher during the jökulhlaup, representing a 20% increase in the average DIC flux compared to the river's 'neutral' state. The average jökulhlaup daily fluxes for Na, Ca, Mg, and Sr are all over 3 times higher than background average fluxes, representing 9–14% increases in the mean daily flux compared to background values (Table 3).

Jökulhlaups are important components of the chemical and physical denudation of Iceland. While the flood measured in this study was minor, previous events have been 1000s times larger in magnitude. These floods are particularly important for the particulate flux, as sediment transport is heavily dependent on runoff (Eiriksdottir et al., 2013a). Nanoparticles and colloids are also integral to increased element fluxes in rivers during eruptions (Tepe and Bau, 2014). The ratio of particulate to dissolved flux of jökulhlaups in southern Iceland has been shown to be 2–6 orders of magnitude greater than global average ratios (Oelkers et al., 2011; Galezka et al., 2014), with the effect more pronounced for trace elements. This has important implications for the estimations of fluvial fluxes of elements to the oceans, particularly for poorly soluble elements. Given that the transport of most elements is dominantly in particulate form (Oelkers et al., 2011, 2012), and that further reactions in saline water represent a considerable further flux of material (Pearce et al., 2013; Jones et al., 2014), basing flux estimates purely on spot samples of dissolved constituents seems imprudent at best. An accurate assessment of such element fluxes is of key interest, as their input to the oceans constrains biological activity and the formation of carbonates, both of which interplay with the global carbon cycle (Gislason et al., 2006a).

Table 2
Average discharge and selected mean element concentrations for Skálm, Skaftá, rivers from northeast Iceland (Eiriksdottir et al., 2013a) and selected global rivers (Gaillardet et al., 1999). The values for Jökulsá í Fljótsdal are taken at Hóll, and at Hjarðarhagi for Jökulsá á Dal (Eiriksdottir et al., 2013a, 2013b).

River	Discharge km ³ /yr	Si μmol/L	Na μmol/L	K μmol/L	Ca μmol/L	Mg μmol/L	Fe μmol/L	Al μmol/L	Cl μmol/L	SO ₄ μmol/L	F μmol/L	DIC ^a mmol/L
Skálm	–	567	526	26	223	164	1.6	1.5	180	112	–	–
Skaftá	1.6	293	354	10	187	103	3.1	3.0	74	71	8.2	0.75
Lagarfljót	3.8	145	131	12	136	82	0.1	0.2	71	22	1.7	0.43
Jökulsá í Fljótsdal	1.1	151	170	6	230	76	0.3	0.4	45	53	3.1	0.68
Jökulsá á Dal	4.7	158	224	9	138	69	0.2	0.6	43	18	3.1	0.55
Grímsá	0.9	160	130	7	141	65	0.3	0.2	78	34	1.6	0.40
Fjarðará	0.1	110	128	4	47	42	0.2	0.1	97	12	0.6	0.20
Fellsá	0.3	152	110	4	70	50	0.1	0.2	58	8	1.0	0.31
Amazon	6590	115	80	21	135	37			61	47		0.34
Changjiang	928	108	222	36	973	292			151	164		2.31
Congo–Zaire	1200	157	96	43	56	59			37	15		0.26
Danube	207	69	739	51	1473	1117			1509	660		3.33
Ganges	493	128	417	67	580	267			143	83		1.95
Lena	525	97	196	18	428	210			343	142		0.87
Mississippi	580	127	478	72	850	366			294	266		1.90
Nile	83	213	2261	200	775	576			1257	542		2.85
Orinoco	1135	105	64	17	65	27			25	24		0.16
St. Lawrence	337	40	239	35	750	247			214	146		1.66

^a Numbers in italics are molar concentrations of HCO₃, assumed to be the same as total dissolved inorganic carbon (DIC).

Table 3

Calculated mean dissolved fluxes for selected elements in Skaftá River. F_{tot} denotes the mean flux for the whole installation period, $F_{\text{jök}}$ refers to the mean element fluxes during the jökulhlaup affected period (19–28 Jan. 2014), and F_{neut} is the mean fluxes from the river in 'neutral' state (13 Nov. 2013–18 Jan. 2014 and 29 Jan.–6 July 2014).

	Si	Na	K	Ca	Mg	Fe	Al	Sr	Mn	Ti	Cl	SO ₄	F	DIC
F_{tot} (t/day)	34.72	9.90	1.66	31.6	10.47	0.994	0.436	0.042	0.028	0.151	10.96	28.29	0.743	50.8
$F_{\text{jök}}$ (t/day)	68.64	30.46	3.22	129.1	32.20	1.038	0.556	0.155	0.203	0.154	16.33	35.86	0.651	269.2
F_{neut} (t/day)	33.36	9.08	1.60	27.7	9.60	0.993	0.431	0.037	0.021	0.151	10.71	27.94	0.748	42.1
$F_{\text{tot}}/F_{\text{neut}}$	1.04	1.09	1.04	1.14	1.09	1.00	1.01	1.12	1.33	1.00	1.02	1.01	0.99	1.21
$F_{\text{jök}}/F_{\text{neut}}$	2.06	3.35	2.02	4.66	3.35	1.05	1.29	4.14	9.66	1.02	1.52	1.28	0.87	6.40

4.4. Further uses for continuous osmotic sampling

Despite the challenges encountered, the robustness and simplicity of the sampler design means that this is a cheap and effective way for monitoring a water body that could be deployed in a number of environments with considerable success. The samplers are also capable of monitoring other volcanic phenomena, including thermal springs, geysers, wells, and ground water, providing the temperature ranges stays above 0 °C and the conditions allow for the safe installation and retrieval of the samplers. Some of the rubber fittings may begin to degrade at high temperatures or under very acidic conditions, but otherwise their deployment is versatile. Thus, the results of this study indicate that their deployment could provide insights into volcanic degassing and element fluxes in a wide variety of settings, particularly in remote locations.

The osmotic samplers were deployed with the initial aim of contributing towards improving early warning systems around subglacial volcanoes. This method of data collection, by nature being sample based rather than sensor based, has its limitations in terms of being able to provide pre-emptive evidence of an impending eruption. The sampler must be collected, transported, and prepared for analysis, which at the current deployment sites would take a minimum of one day if the warning was immediate, with a further week to conduct all of the analyses performed here. This approach may work for studying prolonged unrest at volcanoes such as the ongoing eruption at Holuhraun since August 2014, but it will be insufficient for sudden jökulhlaups or in monitoring volcanoes such as Hekla that historically have had a short interval between onset of unrest and eruption. However, there is a strong potential for osmotic samplers to be used in conjunction with other monitoring techniques such as seismicity and hydrology to contribute to ongoing volcanological monitoring systems and in the understanding of events after they have happened.

5. Conclusions

The deployment of osmotic samplers in Icelandic rivers in southern Iceland has been shown to deliver accurate and detailed data in relatively turbid conditions. These samplers are a cheap and effective means of continuous sampling, offering comprehensive data without the costs normally associated with such thorough chemical monitoring. The daily-averaged samples offer considerably more detail than from spot samples, even during periods when the collection of spot samples is intensive. Moreover, there is no bias towards conditions that suit sampling, such as fair weather and daylight hours. The level of detail offered by this sampling method allows discreet events to be recognised, such as storms bringing in sea-spray into a catchment, the release of transition metals during ground thaw, and small to large discharges from subglacial lakes. Continuous sampling is important when estimating elemental fluxes in fluvial systems, especially for immobile elements such as Mn. These samplers have further use to both hydrological and volcanic sciences. When used in conjunction with other monitoring techniques, these samplers have the potential to be used to understand volcanic processes during times of unrest. There is also the potential to expand their usage to include other water bodies influenced by volcanic processes, such as wells, groundwater, springs, and

geysers. It is our hope that their usage will become more widespread, given the successful deployment in this study.

Acknowledgements

Our thanks go to Peter Wynn and another anonymous reviewer for providing thorough and constructive reviews, and to Alessandro Aiuppa for handling this manuscript as editor. Rósa Ólafsdóttir, Eyþór Valdimarsson, Christian Grimm, Rebecca Neely, Sylviane Lebon, Eydís Eiríksdóttir, Jörunn Harðadóttir, Óðinn Þórarinnsson, Gunnar Sigurdsson, Matthew Roberts, and Reynir Ragnarsson are warmly thanked for their assistance. Morgan Jones, Iwona Gałeczka, and Athanasios Gkritzalis-Papadopoulos were funded through FutureVolc, EU FP7 Contract No. 308377. Morgan Jones is currently supported by the Research Council of Norway through its Centres of Excellence funding scheme, project number 223272.

Appendix A. Supplementary data

Supplementary data to this article can be found online at <http://dx.doi.org/10.1016/j.jvolgeores.2014.12.018>.

References

- Aiuppa, A., Allard, P., D'Alessandro, W.D., Michel, A., Parello, F., Treuil, M., Valenza, M., 2000. Mobility and fluxes of major, minor and trace metals during basalt weathering and groundwater transport at Mt. Etna volcano (Sicily). *Geochim. Cosmochim. Acta* 64, 1827–1841.
- Aiuppa, A., Moretti, R., Federico, C., Giudice, G., Gurrieri, S., Liuzzo, M., Papale, P., Shinohara, H., Valenza, M., 2007. Forecasting Etna eruptions by real-time observation of volcanic gas composition. *Geology* 35 (12), 1115–1118.
- Alho, P., Russell, A.J., Carrivick, J.L., Käyhkö, J., 2005. Reconstruction of the largest Holocene jökulhlaup within Jökulsá á Fjöllum, NE Iceland. *Quat. Sci. Rev.* 24 (22), 2319–2334.
- Arnórsson, S., Andrésdóttir, A., 1995. Processes controlling the distribution of B and Cl in natural waters in Iceland. *Geochim. Cosmochim. Acta* 59, 4125–4146.
- Arsouze, T., Dutay, J.-C., Lacan, F., Jeandel, C., 2009. Reconstructing the Nd oceanic cycle using a coupled dynamical–biogeochemical model. *Biogeosciences* 6, 1–18.
- Björnsson, H., 1977. The cause of jökulhlaups in the Skaftá River, Vatnajökull. *Jökull* 27, 71–77.
- Björnsson, H., 2003. Subglacial lakes and jökulhlaups in Iceland. *Glob. Planet. Chang.* 35 (3–4), 255–271.
- Burgisser, A., Scaillet, B., Harshvardhan, 2008. Chemical patterns of erupting silicic magmas and their influence on the amount of degassing during ascent. *J. Geophys. Res.* B Solid Earth 113 (12), B12204.
- Dickey, T., Frye, D., Jannasch, H.W., Boyle, E., Knap, A.H., 1997. Bermuda sensor system testbed. *Sea Technol.* 38, 81–86.
- Duffell, H.J., Oppenheimer, C., Pyle, D.M., Galle, B., McGonigle, A.J.S., Burton, M.R., 2003. Changes in gas composition prior to a minor explosive eruption at Masaya volcano, Nicaragua. *J. Volcanol. Geotherm. Res.* 126 (3–4), 327–339.
- Edmonds, M., 2008. New geochemical insights into volcanic degassing. *Philos. Trans. R. Soc. A Math. Phys. Eng. Sci.* 366 (1885), 4559–4579.
- Eiríksdóttir, E.S., Gíslason, S.R., Oelkers, E.H., 2013a. Does temperature or runoff control the feedback between chemical denudation and climate? Insights from NE Iceland. *Geochim. Cosmochim. Acta* 107, 65–81.
- Eiríksdóttir, E.S., Gíslason, S.R., Snorrason, Á., Harðadóttir, J., Þorlákssdóttir, S.B., Sveinbjörnsdóttir, Á.E., Neely, R.A., 2013b. Efnasamsetning, rennsli og aurburður straumvatna á Austurlandi X.
- Eiríksdóttir, E.S., Neely, R.A., Þorlákssdóttir, S.B., Gíslason, S.R., 2014. Efnasamsetning, rennsli og aurburður Norðurár í Norðurárdal III.
- Elfesen, S.Ó., Snorrason, Á., Haraldsson, H., Gíslason, S.R., Kristmannsdóttir, H., 2002. Real-time monitoring of glacial rivers in Iceland. In: Snorrason, Á., Finnsdóttir, H.P., Moss, M. (Eds.), *The Extremes of the Extremes: Extraordinary Floods, Proceedings of Reykjavík Symposium*. IAHS, Reykjavík, Iceland, pp. 199–204.

- Flaathen, T.K., Gislason, S.R., 2007. The effect of volcanic eruptions on the chemistry of surface waters: the 1991 and 2000 eruptions of Mt. Hekla, Iceland. *J. Volcanol. Geotherm. Res.* 164 (4), 293–316.
- Gaillardet, J., Dupré, B., Louvat, P., Allègre, C., 1999. Global silicate weathering and CO₂ consumption rates deduced from the chemistry of large rivers. *Chem. Geol.* 159, 3–30.
- Galeczka, I., Oelkers, E.H., Gislason, S.R., 2014. The chemistry and element fluxes of the July 2011 Múlaákvísl and Kaldakvísl glacial floods, Iceland. *J. Volcanol. Geotherm. Res.* 273, 41–57.
- Geirsdóttir, Á., Hardardóttir, J., Sveinbjörnsdóttir, Á.E., 2000. Glacial extent and catastrophic meltwater events during the deglaciation of Southern Iceland. *Quat. Sci. Rev.* 19 (17–18), 1749–1761.
- Gislason, S., Snorrason, Á., Kristmannsdóttir, H., Sveinbjörnsdóttir, Á., Torsander, P., Ólafsson, J., Castet, S., Dupré, B., 2002. Effects of volcanic eruptions on the CO₂ content of the atmosphere and the oceans: the 1996 eruption and flood within the Vatnajökull Glacier, Iceland. *Chem. Geol.* 190, 181–205.
- Gislason, S., Oelkers, E., Snorrason, Á., 2006a. Role of river-suspended material in the global carbon cycle. *Geology* 34 (1), 49–52.
- Gislason, S.R., Snorrason, Á., Ingvarsson, G.B., Eiríksdóttir, E.S., Sigfússon, B., Flaathen, T.K., Camargo, L.G.Q., Elefsen, S.Ó., Harðardóttir, J., Þorlákssdóttir, S.B., Torssander, P., 2006b. Chemistry and Discharge of Rivers Within the Skaftá Catchment From 2002 to 2006. RH-04-2006. Science Institute, Reykjavík Iceland.
- Gkritzalis-Papadopoulos, A., Palmer, M.R., Mowlem, M.C., 2012a. Adaptation of an osmotically pumped continuous in situ water sampler for application in riverine environments. *Environ. Sci. Technol.* 46, 7293–7300.
- Gkritzalis-Papadopoulos, A., Palmer, M.R., Mowlem, M.C., 2012b. Combined use of spot samples and continuous integrated sampling in a study of storm runoff from a lowland catchment in the south of England. *Hydrol. Process.* 26, 297–307.
- Gudmundsson, M.T., Sigmundsson, F., Björnsson, H., 1997. Ice–volcano interaction of the 1996 Gjalp subglacial eruption, Vatnajökull, Iceland. *Nature* 389 (6654), 954–957.
- Gudmundsson, M.T., Larsen, G., Höskuldsson, Á., Gylfason, Á.G., 2008. Volcanic hazards in Iceland. *Jökull* 58, 251–268.
- Icelandic Meteorological Office, 2013. Delivery of Data from the Hydrological Database, No. 2013-06-11/01.
- Icelandic Meteorological Office, 2014a. Delivery of Data from the Hydrological Database, No. 2014-02-13/01.
- Icelandic Meteorological Office, 2014b. Delivery of Data From the Hydrological Database, No. 2014-08-15/02.
- Jannasch, H.W., Wheat, C.G., Plant, J.N., Kastner, M., Stakes, D.S., 2004. Continuous chemical monitoring with osmotically pumped water samplers: OsmoSampler design and applications. *Limnol. Oceanogr. Methods* 2, 102–113.
- Johnson, K.S., Jannasch, H.W., 1994. Analytical chemistry under the sea surface: monitoring ocean chemistry in situ. *Naval Res. Rev.* 46, 4–12.
- Jones, M.T., Hembury, D.J., Palmer, M.R., Tonge, B., Darling, G., Loughlin, S.C., 2011. The weathering and element fluxes from active volcanoes to the oceans: a Montserrat case study. *Bull. Volcanol.* 73 (3), 207–222.
- Jones, M.T., Pearce, C.R., Jeandel, C., Gislason, S.R., Eiríksdóttir, E.S., Mavromatis, V., Oelkers, E.H., 2012a. Riverine particulate material dissolution as a significant flux of strontium to the oceans. *Earth Planet. Sci. Lett.* 355–356, 51–59.
- Jones, M.T., Pearce, C.R., Oelkers, E.H., 2012b. An experimental study of the interaction of basaltic particulate material and seawater. *Geochim. Cosmochim. Acta* 77, 108–120.
- Jones, M.T., Gislason, S.R., Burton, K.W., Pearce, C.R., Mavromatis, V., Pogge von Strandmann, P.A.E., Oelkers, E.H., 2014. Quantifying the impact of riverine particulate dissolution in seawater on ocean chemistry. *Earth Planet. Sci. Lett.* 395, 91–100.
- Kaasalainen, H., Stefánsson, A., 2012. The chemistry of trace elements in surface geothermal waters and steam, Iceland. *Chem. Geol.* 330–331, 60–85.
- Kristmannsdóttir, H., Björnsson, A., Pálsson, S., Sveinbjörnsdóttir, Á.E., 1999. The impact of the 1996 subglacial volcanic eruption in Vatnajökull on the river Jökulsá á Fjöllum, North Iceland. *J. Volcanol. Geotherm. Res.* 92 (3–4), 359–372.
- Lacan, F., Jeandel, C., 2005. Neodymium isotopes as a new tool for quantifying exchange fluxes at the continent–ocean interface. *Earth Planet. Sci. Lett.* 232, 245–257.
- Larsen, G., 2000. Holocene eruptions within the Katla volcanic system, South Iceland: characteristic and environmental impact. *Jökull* 49, 1–28.
- Maizels, J., 1997. Jökulhlaup deposits in proglacial areas. *Quat. Sci. Rev.* 16 (7), 793–819.
- Marteinsonn, V.T., Runarsson, A., Stefánsson, A., Thorsteinsson, T., Johannesson, T., Magnusson, S.H., Reynisson, E., Einarsson, B., Wade, N., Morrison, H.G., Gaidos, E., 2013. Microbial communities in the subglacial waters of the Vatnajökull ice cap, Iceland. *ISME J.* 7 (2), 427–437.
- Moretti, R., Arienzo, L., Civetta, L., Orsi, G., Papale, P., 2013. Multiple magma degassing sources at an explosive volcano. *Earth Planet. Sci. Lett.* 367, 95–104.
- Oelkers, E.H., Gislason, S.R., Eiríksdóttir, E.S., Jones, M.T., Pearce, C.R., Jeandel, C., 2011. The role of riverine particulate material on the global cycles of the elements. *Appl. Geochem.* 26, S365–S369.
- Oelkers, E.H., Gislason, S.R., Eiríksdóttir, E.S., Jones, M.T., Pearce, C.R., Jeandel, C., 2012. Riverine particulate material dissolution in seawater and its implications for the global cycles of elements. *Compt. Rendus Geosci.* 344, 646–651.
- Óladóttir, B.A., Sigmarsson, O., Larsen, G., Thordarson, T., 2008. Katla volcano, Iceland: magmatic composition, dynamics and eruption frequency as recorded by Holocene tephra layers. *Bull. Volcanol.* 70, 475–493.
- Old, G.H., Lawler, D.M., Snorrason, Á., 2005. Discharge and suspended sediment dynamics during two jökulhlaups in the Skaftá river, Iceland. *Earth Surf. Process. Landf.* 30, 1441–1460.
- Pearce, C.R., Jones, M.T., Oelkers, E.H., Pradoux, C., Jeandel, C., 2013. The effect of particulate dissolution on the neodymium (Nd) isotope and Rare Earth Element (REE) composition of seawater. *Earth Planet. Sci. Lett.* 369–370, 138–147.
- Roggensack, K., Hervig, R.L., McKnight, S.B., Williams, S.N., 1997. Explosive basaltic volcanism from Cerro Negro volcano: influence of volatiles on eruptive style. *Science* 277, 1639–1642.
- Russell, A.J., Roberts, M.J., Fay, H., Marren, P.M., Cassidy, N.J., Tweed, F.S., Harris, T., 2006. Icelandic jökulhlaup impacts: implications for ice-sheet hydrology, sediment transfer and geomorphology. *Geomorphology* 75 (1–2), 33–64.
- Russell, A.J., Duller, R., Mountney, N.P., 2010. 11 volcanogenic jökulhlaups (glacier outburst floods) from Mýrdalsjökull: impacts on proglacial environments. *Dev. Quat. Sci.* 13, 181–207.
- Sigvaldason, G.E., 1963. Influence of geothermal activity on the chemistry of three glacial rivers in southern Iceland. *Jökull* 13, 10–17.
- Sigvaldason, G.E., 1965. The Grímsvötn area. Chemical analysis of jökulhlaup water. *Jökull* 15, 125–128.
- Singh, S.P., Singh, S.K., Goswami, V., Buhushan, R., Rai, V.K., 2012. Spatial distribution of dissolved neodymium and ϵ Nd in the Bay of Bengal: role of particulate matter and mixing of water masses. *Geochim. Cosmochim. Acta* 94, 38–56.
- Snorrason, Á., Jónsson, P., Sigurdsson, O., Pálsson, S., Árnason, S., Víkingsson, S., Kaldal, I., 2002. November 1996 Jökulhlaup on Skeidarársandur outwash plain, Iceland. In: Martin, P., Baker, V.R., Garzón, G. (Eds.), *Flood and Megaflood Processes and Deposits: Recent and Ancient Examples*. Blackwell Science, Oxford, pp. 55–67.
- Stefánsdóttir, M., Gislason, S.R., 2005. The erosion and suspended matter/seawater interaction during and after the 1996 outburst flood from the Vatnajökull Glacier, Iceland. *Earth Planet. Sci. Lett.* 237, 433–452.
- Tepe, N., Bau, M., 2014. Importance of nanoparticles and colloids from volcanic ash for riverine transport of trace elements to the ocean: evidence from glacial-fed rivers after the 2010 eruption of Eyjafjallajökull Volcano, Iceland. *Sci. Total Environ.* 488/489, 243–251.
- Theeuwes, F., Yum, S.I., 1976. Principles of the design and operation of generic osmotic pumps for the delivery of semisolid or liquid drug formulations. *Ann. Biomed. Eng.* 4, 343–353.
- Thordarson, T., Larsen, G., 2007. Volcanism in Iceland in historical time: volcano types, eruption styles and eruptive history. *J. Geodyn.* 43 (1), 118–152.
- Tómasson, H., 1996. The jökulhlaup from Katla in 1918. *Ann. Glaciol.* 22, 249–254.
- Varekamp, J.C., 2008. The volcanic acidification of glacial Lake Caviahue, Province of Neuquen, Argentina. *J. Volcanol. Geotherm. Res.* 178, 184–196.
- Waitt, R.B., 2002. Great Holocene floods along Jökulsá á Fjöllum, north Iceland. In: Martin, P., Baker, V.R., Garzón, G. (Eds.), *Flood and Megaflood Processes and Deposits. Recent and Ancient Examples*. Blackwell Science, Oxford, pp. 37–51.
- Zóphóníasson, S., 2010. Rennslí í ám á vatnsárinu 2009/2010. Veðurstofa Íslands.